Intermittent turbulence in a many-body system

Guram Gogia, Wentao Yu, and Justin C. Burton
Department of Physics, Emory University, Atlanta, Georgia 30322, USA

(Received 15 January 2020; revised manuscript received 5 May 2020; accepted 11 May 2020; published 29 May 2020)

In natural settings, intermittent dynamics are ubiquitous and often arise from a coupling between external driving and spatial heterogeneities. A well-known example is the generation of transient, turbulent "puffs" in fluid flow through a pipe with rough walls. Here we show how similar dynamics can emerge in a discrete, crystalline system of particles driven by noise. Polydispersity in particle masses leads to localized vibrational modes that effectuate a transition to a gaslike phase. A minimal model for the evolution of the system's mechanical energies exhibits quasicyclic oscillations, and a single, dimensionless number captures the essential features of the intermittent dynamics, analogous to the Reynolds number for pipe flow.

DOI: 10.1103/PhysRevResearch.2.023250

I. INTRODUCTION

The dynamics of complex systems that are driven away from equilibrium are usually characterized by minor fluctuations around some steady state, which are abruptly punctuated by a "big jump" [1], leading to a dramatically different state. For example, the climate oscillates between hot and cold regimes over millennia [2], lakes switch between high- and low-nutrient regimes on decadal timescales [3], and rain showers pop up for a few minutes during summer afternoons. Additionally, in spatially extended complex "ecologies," such as vegetation [4] and power grids [5], spatiotemporal intermittency often emerges due to a coupling between external random forcing and the underlying structure.

A classical physical example of intermittent dynamics is transitional pipe flow [6], where laminar fluid flow develops spatially disordered and transient turbulent puffs for intermediate flow velocities. Since laminar flow in a pipe is linearly stable for all Reynolds numbers (Re) [7], the emergence of turbulence requires a finite disturbance, such as rough walls [8] or other localized perturbations [9,10]. Despite tremendous progress in experiment [11] and theory [12–15] to capture the statistical properties of turbulence, the exact mechanism of cooperation between structural perturbations and the fluid flow has remained an elusive goal for the last 140 years. The main challenge, as in many other complex systems, lies in relating the local spatiotemporal interactions to the global emergent behavior.

Here we illustrate this connection in a simple, many-body system that manifests intermittent "turbulence." A spatially extended, horizontal layer of charged particles, forced vertically by white noise, continuously switches between crystalline (laminar) and gaslike (turbulent) states. Particle polydispersity leads to spatially localized vibrational modes that are necessary for these intermittent, big jumps to occur. Upon excitation, these localized modes nonlinearly couple to other vibrational modes in the system and redistribute the energy. Furthermore, we introduce a minimal model for the evolution of the total mechanical energy in the vertical and horizontal directions, reminiscent of stochastic predator-prey systems used to describe turbulence [14]. In both the simulation and the model, a single dimensionless number that incorporates external driving, dissipation, and disorder, successfully predicts the intermittent dynamical regime.

II. EXPERIMENTS

The work described here was primarily motivated by recent experimental observations of emergent, intermittent dynamics in a quasi-two-dimensional dusty plasma crystal [16]. Dusty plasmas, unlike their overdamped counterpart (colloidal suspensions) [17,18], obey underdamped dynamics due to their low pressure environment. Inertia often leads to complex, nonlinear dynamics in continuous media, and dusty plasmas provide an unique opportunity to study the role of inertia in emergent, many-body dynamics by visualizing the motion of individual constituents [19–22].

In the experiments, hundreds of electrostatically levitated microspheres formed a single crystalline layer with hexagonal symmetry. Below a threshold pressure, the center-of-mass of the layer oscillated in the z direction [the "laminar" state, Fig. 1(a)]. On minutes-long timescales, the layer intermittently melted and formed a gaslike, "turbulent," state [Fig. 1(b)]. Figure 1(c) shows the average kinetic energy per particle in the xy imaging plane. Throughout the system's evolution, the duration of laminar states varied more strongly than the duration of turbulent states.

The system is inherently nonequilibrium; energy is sourced from the plasma environment, leading to large-amplitude oscillations of each particle in z [23–26]. However, large amplitude oscillations were not sufficient to facilitate the tran-

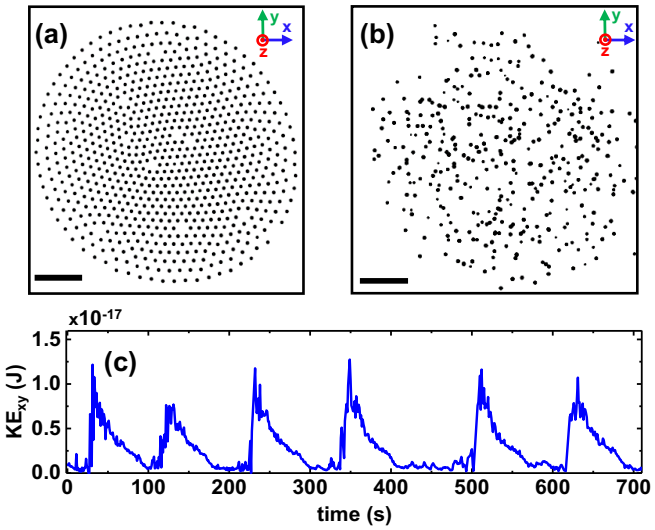

FIG. 1. Images from an experiment showing both the (a) crystalline and (b) gaslike states in a system comprised of 751 melamine formaldehyde spherical particles (density = 1510 kg/m^3, averageradius = 4.73 μm). The scale bars correspond to 5 mm. (c) Over the course of minutes, the system switches between these two states, as evidenced by sharp increases in the horizontal kinetic energy per particle. More details can be found in Gogia *et al.* [16].

sition to the turbulent state. Importantly, the accompanying numerical simulations indicated that intermittent dynamics could only emerge if the particles have some finite size variation. This quenched disorder lead to localized melting, which rapidly redistributed the kinetic energy in the system. Here we generalize these results and identify the key ingredients for this class of intermittent, turbulent dynamics in a many-body system.

III. NUMERICAL SIMULATIONS

We used a custom molecular dynamics code to simulate N particles that interact via a finite-ranged pair potential $U(r) = U_0\lambda e^{-r/\lambda}/r$, where U_0 is the characteristic energy scale, r is the particle separation, and λ is the screening length. The particles are spatially confined vertically and horizontally through harmonic potentials $k_v z^2/2$ and $k_h(x^2+y^2)/2$, where k_v and k_h are the respective spring constants [Fig. 2(a)]. Particles were initially placed at random locations in the xy plane and then quenched to the nearest local potential energy minimum using the FIRE algorithm [27]. In addition, we introduce two nonconservative forces: a hydrodynamic drag force $\vec{\mathbf{F}}_d = -\gamma m\vec{\mathbf{v}}$, where γ is the dissipation rate, m is the particle mass, and $\vec{\mathbf{v}}$ is the particle velocity. To simulate vertical oscillations, we used a spatially uniform Langevin force in the z direction, $\vec{\mathbf{F}}_s = \hat{\mathbf{z}}w(t)\sqrt{m\phi/\Delta t}$, where $w(t)$ is a Wiener process with zero mean and unit standard deviation, ϕ is the power delivered by the noise, and Δt is the simulation time step. The particle positions and velocities were advanced in time using velocity-Verlet integration. With these parameters, we identified a characteristic mass (m), length (λ), and time ($\sqrt{m/k_\mathrm{h}}$) scale in the system. In what follows, all variables have been scaled by these units.

There are two equilibrium conditions that are necessary for the appearance of intermittent dynamics in this system. First, the confinement should be anisotropic so that there is a separation of normal mode frequencies associated with horizontal (xy) and vertical (z) motion. When $k_\mathrm{h} \ll k_\mathrm{v}$, the vertical modes can store a significant amount of mechanical energy without strong coupling to the horizontal modes. This is analogous to wall-bounded, uniaxial, laminar fluid flows, where the majority of kinetic energy is stored in one degree of freedom. When $k_\mathrm{v} \sim k_\mathrm{h}$, we found that the two-dimensional layer of particles would buckle into the z direction (Fig. S2 [28]). Buckled, three-dimensional systems never displayed intermittent dynamics because the vertical and horizontal modes are mixed.

Second, there must be some degree of quenched disorder to facilitate energy transfer from vertical to horizontal modes. Quenched disorder, in the form of rough walls, is also necessary to initiate transient turbulent puffs in pipe flow [29]. To accomplish this in our simulations, the particle masses were chosen from a Gaussian distribution with mean m and coefficient of variation c_v. If the particles had identical masses, the stochastic forcing would simply result in vertical motion of the system's center-of-mass. As we will show, quenched disorder leads to the appearance of localized vibrational modes where neighboring particles can oscillate out-of-phase.

Under stochastic forcing, the intermittent dynamics manifest as punctuated cascades of energy from the vertical (z) to the horizontal directions (xy). An example of this can be seen in the accompanying supplemental movie [28]. The transition to the gaslike state is rather abrupt since a copious amount of excess energy can be stored in the vertical oscillations. This is illustrated by the time series of the fractional horizontal kinetic energy $\Delta_{xy} \equiv KE_{xy}/(KE_z + KE_{xy})$, shown in Fig. 2(b). Laminar, crystalline states correspond to $\Delta_{xy} \ll 1$, and gaslike, turbulent states correspond to $\Delta_{xy} \lesssim 2/3$, where the upper limit corresponds to energy equipartition among the degrees of freedom. Intermittency is distinguished by sharp increases in Δ_{xy}, often separated by long periods of quiescence [Figs. S3(a) and S3(b)].

We quantified the extent of intermittency by taking the integral of the amplitude of Fourier transforms of Δ_{xy} over low frequencies, as described in the Supplemental Material and shown in Fig. S3(c) [28]. We define this quantity as the *switching intensity*, in alignment with Gogia *et al.* [16]. Notably, intermittent dynamics were only observed for a small range of parameters. This is illustrated by the heat map of the switching intensity in Fig. 2(c), where a distinct regime of large switching intensity can be observed, and is characterized by an inverse relationship between c_v and ϕ. Too much disorder or stochastic forcing leads to a perpetually turbulent, gaslike state, and too little leads to a laminar, coherently oscillating crystalline state.

The dynamics in this system undeniably arise from its nonequilibrium and nonlinear nature. Nevertheless, a detailed analysis of the harmonic vibrational modes can shed light on how quenched disorder facilitates switching between states. We used dynamical matrix formalism to calculate the normal

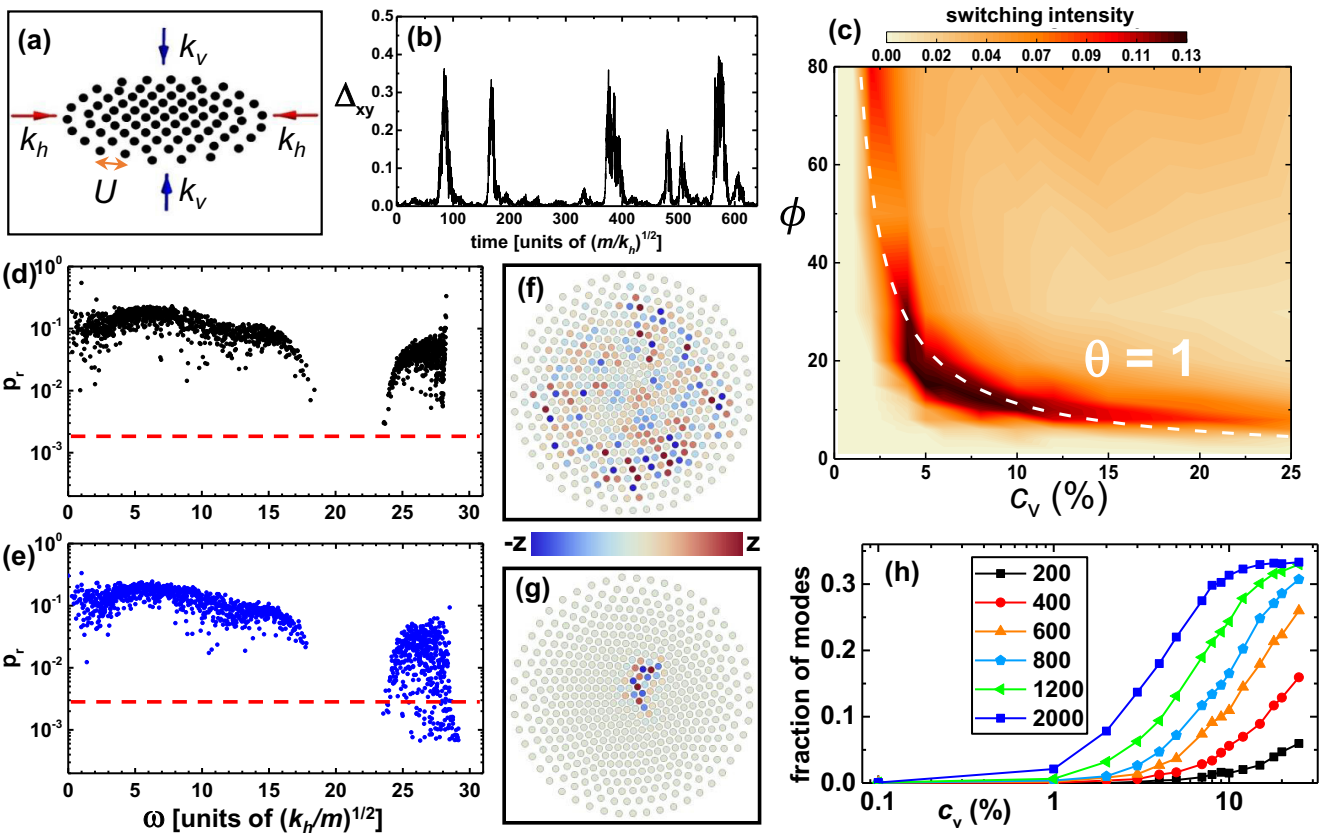

FIG. 2. (a) In the simulations, a single layer of interacting particles is confined horizontally and vertically by harmonic potentials. (b) Temporal evolution of the fractional kinetic energy Δ_{xy} for a polydisperse system of $N = 500$ particles with $c_v = 4\%$ driven with $\phi = 20$. The damping rate was $\gamma = 0.2$ and the vertical confinement was $k_v = 800$. (c) Heat map showing switching intensity as a function of c_v and ϕ for systems with $N = 500$ particles, using the same values of γ and k_v as in (b). The dotted line corresponds to $\theta = 1$ [Eq. (4)] and captures the inverse relation between ϕ and c_v. Participation ratio (p_r) vs mode frequency for a monodisperse (d) and a polydisperse (e) system. The dashed red line corresponds to the lowest value of p_r in the monodisperse sample. (f) and (g) Vertical polarization for a high-p_r and low-p_r mode, respectively, in a polydisperse system with $c_v = 4\%$ and $k_v = 800$. (h) Fraction of vertical modes with low-p_r as a function of c_v for different values of k_v, as indicated by the legend.

modes of the system [30–32]. The weighted Hessian matrix K was computed about the local potential energy minimum:

$$K_{ij} = \frac{\partial^2 V}{\partial r_i^\alpha \partial r_j^\beta}, \tag{1}$$

where V is the total potential energy, including the external confining potentials, i and j denote the ith and jth particle, and α and β denote (x, y, z) coordinates. Using the harmonic approximation, Newton's second law yields

$$M\ddot{\vec{x}} + K\vec{x} = 0, \tag{2}$$

where $\vec{\mathbf{x}}$ is the displacement vector of particle positions from equilibrium, and $M = \sqrt{m_i m_j}$. For N particles in three dimensions, M and K are $3N \times 3N$ matrices and x is a $3N \times 1$ vector. The dynamical matrix $D = K/M$ has $3N$ eigenvalues which correspond to squares of the mode angular frequencies and the normalized eigenvectors represent the polarizations of the particle displacements.

In order to characterize the spatial extent of each mode, we calculated the participation ratio p_r for each eigenvector. The quantity p_r characterizes the fraction of particles participating in a given vibrational mode:

$$p_r = \frac{\left(\sum_i |\hat{\mathbf{e}}_{m,i}|^2\right)^2}{N \sum_i |\hat{\mathbf{e}}_{m,i}|^4}, \tag{3}$$

where $\hat{\mathbf{e}}_{m,i}$ is the polarization vector of the ith particle in the mth unit eigenvector. Modes with $p_r \lesssim 1$ represent the collective motion of many particles, whereas the modes with $p_r \ll 1$ correspond to localized modes consisting of a few particles.

Figures 2(d) and 2(e) show p_r versus angular frequency for monodisperse and polydisperse systems, respectively, each comprised of $N = 500$ particles. There are two distinct frequency bands. High frequency modes ($\omega \gtrsim 25$) correspond to vertical motion, and low frequency modes ($\omega < 20$) correspond to horizontal motion. A frequency gap, which is a direct consequence of anisotropic confinement, separates these bands and suppresses coupling between horizontal and vertical modes. A typical extended vertical mode is shown in Fig. 2(f). A small amount of quenched disorder in particle mass ($c_v > 0$) leads to localized modes [Fig. 2(g)] with $p_r \ll 1$ in the vertical frequency band, yet leaves the horizontal frequency band essentially unchanged.

When driven with a spatially uniform (wave vector $k = 0$), stochastic force, only modes with some corresponding $k = 0$ Fourier components can be excited. This can be seen by considering a single massive particle in a crystal of otherwise identical particles. A stochastically driven harmonic oscillator has a peak response at its fundamental frequency. The massive particle will have a lower fundamental frequency, and eventually oscillate out-of-phase with its neighbors. This highly localized vibrational mode will contain a broad spectrum of spatial wave vectors both at high and low k [33], and can potentially couple to external driving at $k = 0$.

These modes are also more susceptible to nonlinear coupling since the relative amplitude of motion between neighboring particles is larger. Consequently, low participation ratio vertical modes serve as the progenitors of the energy cascade from vertical to horizontal degrees of freedom. Such localized imperfections may provide a clear link between external driving, spatial heterogeneities, and intermittent dynamics in a wide variety of systems. Indeed, even though it was clear to Reynolds that wall roughness was instrumental [9], a rigorous connection between wall roughness and intermittent turbulence in pipe flow was only recently established as "roughness-induced criticality" [29].

Furthermore, we quantified the fraction of vibrational modes with p_r below the lowest value for a monodisperse sample ($c_v = 0$), as shown by the dashed red lines in Figs. 2(d) and 2(e). This fraction increased monotonically with the amount of disorder and the ratio of vertical to horizontal confinement k_v/k_h. As illustrated in Fig. 2(h), for strong confinement, the gap between the frequency bands is large and a small amount of disorder can quickly lead to mode localization. For weak confinement, the gap is small or nonexistent and mode localization requires more structural disorder. For all the data shown in Fig. 2(h), intermittency occurs when the fraction of low-p_r modes is approximately 0.07–0.2. In this manner, the linear, equilibrium properties can inform the system's nonequilibrium dynamical response [34].

The inverse relationship between ϕ and c_v shown in Fig. 2(c) suggests that intermittency may be described by an unknown dimensionless quantity. We identified five relevant dimensionless numbers through Buckingham's Pi theorem [35]: c_v, k_v/k_h, $U_0/k_h\lambda^2$, $k_v/m\gamma^2$, and $\phi/k_v\lambda^2\gamma$. c_v characterizes the degree of structural disorder. k_v/k_h and $U_0/k_h\lambda^2$ determine the degree of quasi-two-dimensional confinement. If either number is too small, then the system's equilibrium configuration will be "buckled" into the z direction (Fig. S2 [28]). $k_v/m\gamma^2$ determines the quality factor of underdamped vertical oscillations of a single particle. Lastly, $\phi/k_v\lambda^2\gamma$ is the only number associated with the external forcing. This can be intuited as the amount of noisy power necessary for a stochastic, damped harmonic oscillator to reach an average amplitude λ, $k_v\lambda^2/2 = \phi/4\gamma$. For a single particle driven by noise, we confirmed that the root-mean-squared amplitude scales as $\sqrt{\phi}$ (Fig. S5 [28]). This amplitude threshold will induce rearrangements in the crystalline lattice since the particle spacing is also of order λ, similar to the Lindemann criteria in classical melting [36]. For a thermal, Brownian oscillator, $2\gamma k_B T$ would assume the role of ϕ in our simulations.

We can form a single dimensionless number that describes the system-wide, intermittent dynamics by considering the role of disorder on the vertical oscillations. Since localized modes consist of only a few neighboring particles, we will examine two particles for simplicity. Since each particle has a slightly different mass, their vertical frequencies vary, $\omega_v + \Delta\omega_v = \sqrt{k_v/(m + \Delta m)} \sim \omega_v(1 - c_v/2)$, where $c_v = \Delta m/m$. For $\Delta\omega_v$ to be significant, it must be larger than γ, which determines the broadness of the oscillatory response in frequency space. If γ is too large, the oscillators will be strongly coupled. Thus, by multiplying the stochastic forcing, $\phi/k_v\lambda^2\gamma$, by the disorder in frequency space, $c_v\omega_v/\gamma$, we obtain

$$\theta \equiv \frac{c_v\phi}{\sqrt{k_v m}\lambda^2\gamma^2}. \tag{4}$$

θ characterizes the ratio of energy input to dissipation, modulated by disorder. This is analogous to a "friction factor" in transitional pipe flow that includes the cooperative effects of wall roughness and Reynolds number [29]. For reasonable values of the other dimensionless numbers, intermittent dynamics should occur along contours of constant $\theta \approx 1$, as shown by the white dashed line in Fig. 2(c). Additionally, Figs. S4(a) and S4(b) [28] show heat maps of ϕ vs c_v for different values of k_v, and Fig. S4(c) [28] shows a heat map of ϕ vs γ. In all cases, intermittency is maximized when $\theta \approx 1$.

It is important to note that the expression for θ, Eq. (4), can also predict the regime of intermittent dynamics in the experiments, with one important distinction. The particles in the experiment are not driven by uncorrelated white noise, as in the numerical simulations [16]. In fact, the vertical oscillations are well described by a delayed charging mechanism [23,26], which results in an effective "negative damping" of the particle's motion. Although the driving mechanism is different, in both cases each particle oscillates primarily at its fundamental frequency, so that disorder in particle mass leads to variations in oscillation frequency ($\Delta\omega_v > 0$).

To directly compare to the experiments, it is helpful to rewrite θ in terms of the average vertical oscillation frequency: $\theta = c_v\phi/\omega_v m\lambda^2\gamma^2$. In the experiments [16,26], $\omega_v \approx$ 60–120 Hz, $m \approx 6.7 \times 10^{-13}$ kg, $\gamma \approx 0.7\ \mathrm{s}^{-1}$, $c_v \approx 3.6\%$, and $\lambda \approx 1.9$ mm. An estimate for the equivalent value of ϕ can be obtained by comparing the amplitude of vertical oscillations in the experiment ≈ 0.8–1 mm, with the normalized oscillation amplitude vs ϕ [Fig. S5(a)]. The result is $\phi \approx 3.8 \times 10^{-15}$ W. Putting this all together, we estimate that $0.9 \lesssim \theta \lesssim 1.8$ for the intermittent regime in the experiment. This illustrates that the same dimensionless number can accurately capture the dynamics in the experiment.

IV. MINIMAL MODEL FOR MANY-BODY TURBULENCE

An ecosystem of two or more competing species is an archetypal model for studying oscillations in dynamical systems [37,38]. Conventional predator-prey models consider constant birth and death rates and symmetric "predation" interactions. These conventional models are deterministic and oscillations of predator and prey populations decay to a fixed point. Once a third species is introduced to the system, large-scale fluctuations can arise [39,40]. In some cases, the third species can be food resources for the prey [41]. Quite remarkably, noise can also assume the role of a third species

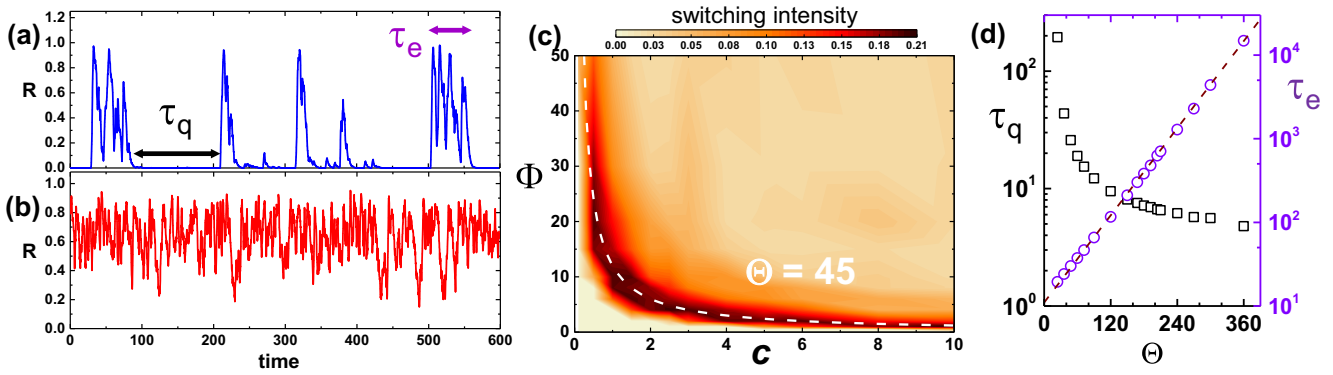

FIG. 3. In the minimal model, the temporal evolution of the fractional horizontal mechanical energy R exhibits intermittent switching for $c = 1$ and $\Phi = 8$ (a), and is perpetually excited for $c = 4$ and $\Phi = 20$ (b). In both panels, $\gamma = 0.5$. (c) Heat map showing the switching intensity, computed by integrating the low-frequency Fourier spectrum of R, as a function of c and Φ with $\gamma = 0.5$. The dotted line corresponds to a constant $\Theta = 45$ and captures the inverse relationship between Φ and c. (d) The mean duration of quiescent (τ_q) and excited (τ_e) states depends strongly on Θ, as computed by varying Φ in Eq. (7) with $\gamma = 0.5$ and $c = 1.5$. The states are separated using a threshold for $A/\langle B\rangle$, as described in the text. The functional form of the dashed line is $11\exp(\Theta/50)$.

and induce quasicyclic oscillations. Environmental and demographic noise terms have been found to induce, *inter alia*, quasicycles in population levels at emergent timescales [42–44]. Outside of biological systems, a three-species framework has been utilized to understand the oscillation of light emission from dust-forming plasmas [45] and intermittent precipitation in climate models [46]. In fact, a stochastic predator-prey model has been instrumental in understanding the statistical features of transitional pipe flow [14].

In our many-body system, we employed a stochastic predator-prey framework to describe the total horizontal mechanical energy (A) as a predator, and the total vertical mechanical energy (B) as a prey to be consumed:

$$\frac{dA}{dt} = -\gamma A + cAB(1 - \sqrt{A/B}), \tag{5}$$

$$\frac{dB}{dt} = -\gamma B - cAB(1 - \sqrt{A/B}) + w(t)\sqrt{B\Phi/\Delta t}. \tag{6}$$

Here we have assumed that kinetic and potential energies are equipartitioned in each direction, so that $A = 2\langle KE_{xy}\rangle$ and $B = 2\langle KE_z\rangle$. The first terms on the right-hand side in (5) and (6) correspond to the power dissipated through hydrodynamic damping, $\sum \vec{\mathbf{F}}_d \cdot \vec{\mathbf{v}} = -\sum \gamma m(v_x^2 + v_y^2 + v_z^2) = -\gamma(A + B)$, where the sum runs over each particle. The second term characterizes predation and obeys energy conservation. The functional form cAB is the lowest-order nonlinear term that captures mutual interactions in common predator-prey models. However, in our minimal model, this coupling term actually arises from energy transfer rates between vertical and horizontal energies, and is derived from classical scattering theory [28]. The constant c controls the coupling strength, and parametrizes the polydispersity in the many-body system. Finally, the third term in Eq. (6) represents the instantaneous power delivered in the vertical direction $\vec{\mathbf{F}}_s \cdot v_z\hat{\mathbf{z}}$, where $v_z \sim \sqrt{B/m}$, Φ is the average power, and Δt is the time step in the simulation. Similar noise terms are commonly used to model demographic stochasticity in ecological systems.

These equations recreate the three observed dynamical regimes. To directly compare with the numerical simulations, we define $R \equiv A/(A + B)$ as the fractional horizontal mechanical energy, in analogy to Δ_{xy} [Fig. 2(b)]. For intermediate values of c and Φ, R exhibits intermittent behavior [Fig. 3(a)], whereas sufficiently increasing either parameter results in a perpetually excited, equipartitioned state ($A \sim B$) [Fig. 3(b)]. The dependence of the switching intensity on both parameters can be seen in Fig. 3(c). The heat map shows that there is a distinct region where intermittent dynamics are maximized.

In a similar manner to the particle-based simulations, this regime can be described by a single dimensionless number,

$$\Theta = c\Phi/\gamma^2, \tag{7}$$

which represents the ratio of the energy input and coupling to dissipation. Intermittent dynamics are maximized for $\Theta \approx 45$ [Fig. 3(c)], in analogy to transitional pipe flow, where intermittent turbulence is observed for intermediate Reynolds numbers ($1700 \lesssim \mathrm{Re} \lesssim 2300$) [47]. To further illustrate how the dynamics are characterized by Θ alone, we show a heat map of Φ vs γ in Fig. S7 [28], where intermittency is also maximized for $\Theta \approx 45$.

The discrepancy between the optimal values of Θ and θ for intermittent dynamics [Eqs. (4) and (7)] stems from the anisotropic confinement in the experiments and numerical simulations, i.e., $k_v/k_h \approx 1000$. This separation of energy scales is necessary to produce a frequency gap between the two sets of vibrational modes [Figs. 2(d) and 2(e)], yet is not represented in the minimal model. Beyond the gap, the energy scale for the vertical oscillations at the inception of gaslike phase is $k_v\lambda^2$. To include this in the minimal model, in accordance with the scaling in Eq. (4), we should make the substitution $c \to c\sqrt{k_v/k_h}$, which would lead to optimal values of Θ closer to unity in Eq. (7). However, this only amounts to a rescaling of the parameters, and does not qualitatively change the dynamical regimes observed in the minimal model.

Lastly, we computed the lifetime statistics of the quiescent (laminar) and excited (turbulent) states in our minimal model. In transitional pipe flow, which is known to exhibit spatiotemporal, critical behavior [48], the lifetime statistics and universality class are related to directed percolation where laminar flow acts as a nonequilibrium absorbing state

[13,14,48–50]. For intermittent turbulence with spatially separated, coexisting, independent puffs, the lifetime of the turbulent state scales superexponentially with Reynolds number [11,14]. We separated the excited and quiescent states in our minimal model using a threshold. Excited states corresponded to $A/\langle B\rangle > 0.02$, where $\langle B\rangle$ represents the average over the entire time series. After the initial thresholding, quiescent periods that are shorter than 3 time units were removed while the two neighboring excited periods were concatenated. The remaining short excited periods that were less than 3 time units are not counted in the distributions. An example of distributions for quiescent and excited lifetimes with $\Theta = 48$ are presented in Fig. S8 [28], where both show exponential tails. The mean lifetime of the excited (turbulent) state scales exponentially with Θ [Fig. 3(d)]. This scaling originates from the memoryless noise driving the system. If our many-body system were spatially extended and could support multiple excited, gaslike regions, we would expect extreme value statistics and subsequently, superexponential behavior [48].

V. SUMMARY

Intermittent dynamics are commonly observed in natural systems but rarely understood. Here we presented a distinct mechanism to promote intermittent dynamics in a tractable, many-body system. A layer of polydisperse, interacting particles, damped by the environment and driven anisotropically by noise, can intermittently transition between "turbulent" and "laminar" states. Spatial heterogeneities, in the form of localized vibrational modes, couple with the external noise to facilitate this transition. In this sense, external noise acts as an engine that drives the system in one direction, and structural heterogeneities act as a rudder that intermittently steer energy into other degrees of freedom.

For the numerical simulations and the minimal model presented here, we derived a single dimensionless number that characterizes the intermittent regime, which agrees well with experiments. The coupling mechanism and associated dimensionless number strongly resemble intermittent turbulence in wall-bounded fluid flow, where the laminar state is punctuated by transient puffs of turbulence due to the finite roughness of the boundaries. Moreover, the minimal model allows us to capture the essential features of the many-body dynamics, and demonstrates an exponential scaling of the lifetimes of the excited states. We hope these results lead to further connections between simple, discrete particle dynamics and natural complex systems.

ACKNOWLEDGMENTS

We acknowledge financial support from the National Science Foundation Grant No. 1455086. We gratefully acknowledge H.-Y. Shih and N. Goldenfeld for stimulating discussions about predator-prey systems. We would like to thank J. Mendez, M. Kawamura, H. Saul, J. Silverberg, A. Roman, I. Nemenman, M. Martini, B. Beal, and B. Doolittle for useful discussions.

[1] N. Goldenfeld and L. P. Kadanoff, Simple lessons from complexity, Science **284**, 87 (1999).

[2] J. R. Petit, J. Jouzel, D. Raynaud, N. I. Barkov, J.-M. Barnola, I. Basile, M. Bender, J. Chappellaz, M. Davis, G. Delaygue, M. Delmotte, V. M. Kotlyakov, M. Legrand, V. Y. Lipenkov, C. Lorius, L. Pépin, C. Ritz, E. Saltzman, and M. Stievenard, Climate and atmospheric history of the past 420,000 years from the Vostok ice core, Antarctica, Nature (London) **399**, 429 (1999).

[3] E. H. van Nes, W. J. Rip, and M. Scheffer, A theory for cyclic shifts between alternative states in shallow lakes, Ecosystems **10**, 17 (2007).

[4] P. D'Odorico, F. Laio, and L. Ridolfi, Vegetation patterns induced by random climate fluctuations, Geophys. Res. Lett. **33**, L19404 (2006).

[5] T. Nesti, A. Zocca, and B. Zwart, Emergent Failures and Cascades in Power Grids: A Statistical Physics Perspective, Phys. Rev. Lett. **120**, 258301 (2018).

[6] B. Eckhardt, T. M. Schneider, B. Hof, and J. Westerweel, Turbulence transition in pipe flow, Annu. Rev. Fluid Mech. **39**, 447 (2007).

[7] M. Lessen, S. G. Sadler, and T.-Y. Liu, Stability of pipe poiseuille flow, Phys. Fluids **11**, 1404 (1968).

[8] J. Nikuradze, Laws of flow in rough pipes, vDI Forschungsheft **4**, 361 (1933).

[9] O. Reynolds, XXIX. An experimental investigation of the circumstances which determine whether the motion of water shall be direct or sinuous, and of the law of resistance in parallel channels, Philos. Trans. R. Soc. London Sect. B **174**, 935 (1883).

[10] B. Hof, A. Juel, and T. Mullin, Scaling of the Turbulence Transition Threshold in a Pipe, Phys. Rev. Lett. **91**, 244502 (2003).

[11] K. Avila, D. Moxey, A. de Lozar, M. Avila, D. Barkley, and B. Hof, The onset of turbulence in pipe flow, Science **333**, 192 (2011).

[12] H. Chaté and P. Manneville, Transition to Turbulence Via Spatio-Temporal Intermittency, Phys. Rev. Lett. **58**, 112 (1987).

[13] D. Barkley, Theoretical perspective on the route to turbulence in a pipe, J. Fluid Mech. **803**, P1 (2016).

[14] H.-Y. Shih, T.-L. Hsieh, and N. Goldenfeld, Ecological collapse and the emergence of travelling waves at the onset of shear turbulence, Nat. Phys. **12**, 245 (2016).

[15] P. Manneville, Transition to turbulence in wall-bounded flows: Where do we stand? Mech. Eng. Rev. **3**, 15-00684 (2016).

[16] G. Gogia and J. C. Burton, Emergent Bistability and Switching in a Nonequilibrium Crystal, Phys. Rev. Lett. **119**, 178004 (2017).

[17] M. Chaudhuri, A. V. Ivlev, S. A. Khrapak, H. M. Thomas, and G. E. Morfill, Complex plasma: The plasma state of soft matter, Soft Matter **7**, 1287 (2011).

[18] A. V. Ivlev, H. Löwen, G. Morfill, and P. C. Royall, *Complex Plasmas and Colloidal Dispersions: Particle-Resolved Studies*

of Classical Liquids and Solids (World Scientific, Singapore, 2012).

[19] L. Couëdel, V. Nosenko, A. V. Ivlev, S. K. Zhdanov, H. M. Thomas, and G. E. Morfill, Direct Observation of Mode-Coupling Instability in Two-Dimensional Plasma Crystals, Phys. Rev. Lett. **104**, 195001 (2010).

[20] A. V. Ivlev, J. Bartnick, M. Heinen, C.-R. Du, V. Nosenko, and H. Löwen, Statistical Mechanics Where Newton's Third Law is Broken, Phys. Rev. X **5**, 011035 (2015).

[21] N. P. Kryuchkov, A. V. Ivlev, and S. O. Yurchenko, Dissipative phase transitions in systems with nonreciprocal effective interactions, Soft Matter **14**, 9720 (2018).

[22] C.-S. Wong, J. Goree, Z. Haralson, and B. Liu, Strongly coupled plasmas obey the fluctuation theorem for entropy production, Nat. Phys. **14**, 21 (2018).

[23] S. Nunomura, T. Misawa, N. Ohno, and S. Takamura, Instability of Dust Particles in a Coulomb Crystal Due to Delayed Charging, Phys. Rev. Lett. **83**, 1970 (1999).

[24] A. A. Samarian, B. W. James, S. V. Vladimirov, and N. F. Cramer, Self-excited vertical oscillations in an rf-discharge dusty plasma, Phys. Rev. E **64**, 025402(R) (2001).

[25] C. Marmolino, Stochastic heating of dust particles in complex plasmas as an energetic instability of a harmonic oscillator with random frequency, Phys. Plasmas **18**, 103701 (2011).

[26] J. M. Harper, G. Gogia, Z. Wu, B. Laseter, and J. C. Burton, The origin of large amplitude oscillations of dust particles in a plasma sheath, arXiv:1908.03138.

[27] E. Bitzek, P. Koskinen, F. Gähler, M. Moseler, and P. Gumbsch, Structural Relaxation Made Simple, Phys. Rev. Lett. **97**, 170201 (2006).

[28] See Supplemental Material at http://link.aps.org/supplemental/10.1103/PhysRevResearch.2.023250 for videos of the simulations and supplemental figures described in the main text.

[29] N. Goldenfeld, Roughness-Induced Critical Phenomena in a Turbulent Flow, Phys. Rev. Lett. **96**, 044503 (2006).

[30] S. Henkes, C. Brito, and O. Dauchot, Extracting vibrational modes from fluctuations: a pedagogical discussion, Soft Matter **8**, 6092 (2012).

[31] A. Bottinelli and J. L. Silverberg, How to: Using mode analysis to quantify, analyze, and interpret the mechanisms of high-density collective motion, Front. Appl. Math. Stat. **3**, 26 (2017).

[32] J. C. Burton and S. R. Nagel, Echoes from anharmonic normal modes in model glasses, Phys. Rev. E **93**, 032905 (2016).

[33] L. E. Silbert, A. J. Liu, and S. R. Nagel, Normal modes in model jammed systems in three dimensions, Phys. Rev. E **79**, 021308 (2009).

[34] D. Mukamel, Phase transitions in nonequilibrium systems, in *Soft and Fragile Matter: Nonequilibrium Dynamics, Metastability and Flow (PBK)*, edited by M. E. Cates and M. R. Evans (SUSSP, Edinburgh, 2000), pp. 237–258.

[35] E. Buckingham, The principle of similitude, Nature (London) **96**, 396 (1915).

[36] F. A. Lindemann, The calculation of molecular vibration frequencies, Phys. Z. **11**, 609 (1910).

[37] A. J. Lotka, Contribution to the theory of periodic reactions, J. Phys. Chem. **14**, 271 (1910).

[38] V. Volterra, *Variazioni e Fluttuazioni Del Numero D'individui in Specie Animali Conviventi* (C. Ferrari, 1926), p. 31.

[39] R. R. Vance, Predation and resource partitioning in one predator–two prey model communities, Am. Nat. **112**, 797 (1978).

[40] M. E. Gilpin, Spiral chaos in a predator-prey model, Am. Nat. **113**, 306 (1979).

[41] C. B. Huffaker, K. B. Shea, and S. Herman, Experimental studies on predation: Complex dispersion and levels of food in an acarine predator-prey interaction, Hilgardia **34**, 305 (1963).

[42] J. V. Greenman and T. G. Benton, The amplification of environmental noise in population models: causes and consequences, Am. Nat. **161**, 225 (2003).

[43] O. N. Bjørnstad, R. M. Nisbet, and J.-M. Fromentin, Trends and cohort resonant effects in age-structured populations, J. Anim. Ecol. **73**, 1157 (2004).

[44] A. J. McKane and T. J. Newman, Predator-Prey Cycles from Resonant Amplification of Demographic Stochasticity, Phys. Rev. Lett. **94**, 218102 (2005).

[45] A. E. Ross and D. R. McKenzie, Predator-prey dynamics stabilised by nonlinearity explain oscillations in dust-forming plasmas, Sci. Rep. **6**, 24040 (2016).

[46] I. Koren and G. Feingold, Aerosol–cloud–precipitation system as a predator-prey problem, Proc. Natl. Acad. Sci. USA **108**, 12227 (2011).

[47] R. R. Kerswell, Recent progress in understanding the transition to turbulence in a pipe, Nonlinearity **18**, R17 (2005).

[48] N. Goldenfeld and H.-Y. Shih, Turbulence as a problem in non-equilibrium statistical mechanics, J. Stat. Phys. **167**, 575 (2017).

[49] Y. Pomeau, Front motion, metastability and subcritical bifurcations in hydrodynamics, Physica D **23**, 3 (1986).

[50] Y. Pomeau, The long and winding road, Nat. Phys. **12**, 198 (2016).